

# Superconducting gap and electron-phonon interaction in MgB<sub>2</sub> thin film studied by point contacts

N. L. Bobrov, P. N. Chubov, Yu. G. Naidyuk\*, L.V. Tyutrina, and I. K. Yanson

*B. Verkin Institute for Low Temperature Physics and Engineering, National Academy of Sciences of Ukraine,  
47 Lenin Ave., 61103, Kharkiv, Ukraine*

W. N. Kang, Hyeong-Jin Kim, Eun-Mi Choi, and Sung-Ik Lee

*National Creative Research Initiative Center for Superconductivity, Department of Physics,  
Pohang University of Science and Technology, Pohang 790-784, South Korea*

(December 2, 2024)

The superconducting gap and electron-phonon interaction (EPI) in a MgB<sub>2</sub> c-axis oriented thin film are investigated by point contacts (PCs). Two order parameters  $\Delta_{small} \approx 2.6$  meV and  $\Delta_{Large} \approx 7.4$  meV have been established, which fairly well correspond to the theoretical gap ratio 1:3. The reconstructed PC EPI function along c-axis has above 30 meV similarities with the phonon DOS, while below 30 meV a pronounced structure is resolved pointing that the low frequency phonon mode can be of importance for pairing. We have also estimated the Fermi velocity  $5 \times 10^7$  cm/s in MgB<sub>2</sub>.

## INTRODUCTION

The compound MgB<sub>2</sub> with graphite-like planes of boron atoms attracts much attention as superconductor with at the present the highest  $T_c \simeq 40$  K for a binary systems [1]. The observation of boron isotope effect [2,3] and examination of electron-phonon coupling [5–10] in MgB<sub>2</sub> are in accordance with the expectations for conventional BCS superconductivity mediated by electron-phonon interaction (EPI). Investigations of the order parameter by tunneling [11–17] and point-contact technique [17–21] confirm that MgB<sub>2</sub> is most likely an *s*-wave superconductor. In all cases the spectra show unambiguous features of an energy gap  $\Delta$  in the density of states (DOS), albeit the results are controversial on the gap width. Values of  $\Delta$  ranging from 2 to 7.5 meV have been reported, pointing out the possibility of an anisotropic or distributed (non-homogeneous) energy gap or even multiple gaps. The latter scenario has been recently recalled by Liu et al. [8] for MgB<sub>2</sub>. The Fermi surface consisting from nearly cylindrical hole sheets arising from quasi-2D boron bands and three dimensional tubular network was considered. The different character of the sheets raises the possibility that each has a distinct gap. The existence of two different energy gaps with the ratio approximately 1:3 being respectively smaller (for the 3D gap) and larger (for the 2D gap) than the standard weak coupling BCS value  $\Delta = 1.76 k_B T_c$  was predicted in [8].

Determination of the Eliashberg function  $\alpha^2 F$  for superconducting systems provides a consistency check of

the phonon-mediated pairing mechanism. In [5–10] the phonon dispersion and DOS, the EPI function  $\alpha^2 F$  and electron-phonon coupling constant  $\lambda$ ,  $T_c$  and isotope effect for MgB<sub>2</sub> have been calculated using different methods and approximation. Estimation of the electron-phonon-coupling strength in MgB<sub>2</sub> [4–9] yields  $\lambda \simeq 1$ . Established by different authors, the phonon DOS and the EPI function have both similarities and differences. The common feature for presented in [6,9,10,22] phonon DOS is the maximum energy of about 100 meV, absence of visible phonon peaks below 30 meV and rich structure with a number of peaks in between 30-100 meV. The main feature of the calculated EPI function is a dominant maximum between 60 and 75 meV arising from in-plane boron E<sub>2g</sub> phonon mode. The precise energy position and shape of the maximum depend on the method of calculation [5,6,8]. The transport EPI function, as shown in [5], mimics the EPI one, although, as mentioned in [8], inter-band anisotropy reduces the transport coupling constant from 1 to 0.5. From both the DC resistivity and optical conductivity measurements [23], even a smaller value of  $\lambda_{tr} = 0.13$  is derived.

However, some neutron inelastic scattering measurements with higher resolution [24,25] revealed a clear maxima in generalized phonon DOS below 30 meV, namely at 16 and 24 meV [24] or 17.5 meV in [25]. Therefore it is an open question whether the only high frequency phonons are responsible for thermodynamic, transport and especially for fascinating SC properties of MgB<sub>2</sub>.

It has been also suggested in [26] that the "multi-gap"

---

\*Corresponding author. e-mail: naidyuk@ilt.kharkov.ua

structure observed in the tunneling spectra [15] can be explained by considering of a low-frequency phonon mode at 17.5 meV, which is revealed in the inelastic neutron scattering experiment [25]. Soft bosonic mode was also exploiting in [27] to describe an upper critical field behavior of MgB<sub>2</sub> within a multi-band Eliashberg model.

Measuring of a nonlinear conductivity of point contacts (PC) between two metals in a direct way allows recovering the EPI function  $\alpha^2 F$  [28], as well as investigating the superconducting (SC) gap [29]. The goal of this report is simultaneous studying of peculiarities of EPI along with SC order parameter of MgB<sub>2</sub> by PC method in order to clarify the mentioned issues, namely, the multigap structure of the order parameter and the peculiarities of EPI function, trying to find their correlation.

## I. EXPERIMENTAL AND RESULTS

We have used the high-quality c-axis oriented MgB<sub>2</sub> thin films grown by a pulsed laser deposition technique [30]. The thin films were grown on (1  $\bar{1}$  0 2) Al<sub>2</sub>O<sub>3</sub> substrates. The typical film thickness was 0.4  $\mu\text{m}$ . The resistivity of the film exhibits a sharp transition at 39 K with a width of  $\sim 0.2$  K from 90% to 10% of the normal state resistivity [31]. The residual resistivity  $\rho_0$  at 40 K is  $\sim 6 \mu\Omega\text{cm}$  and RRR=2.3<sup>1</sup>.

Different contacts were established in situ at liquid <sup>4</sup>He temperatures by touching as prepared surface of the MgB<sub>2</sub> film by the sharpened edge of an Ag counterelectrode, which were cleaned by chemical polishing. By this means the current flow through PCs is preferably along the c-axis. The experimental cell with the samples holder was immersed directly in liquid <sup>4</sup>He to ensure good thermal coupling. Both the differential resistance  $dV/dI$  and  $d^2V/dI^2(V)$  vs  $V$  were registered using a standard lock-in technique. The zero-bias resistance  $R_0$  of investigated contacts ranges from 10 to 1000  $\Omega$  at 4.2 K.

### A. Superconducting gap

According to the Blonder-Tinkham-Klapwijk theory [29] of conductivity of N-c-S metallic junctions (here N is normal metal, c is constriction and S is superconductor) a maximum at zero-bias voltage and a double-minimum structure around  $V \simeq \pm\Delta/e$  in the  $dV/dI$  curves manifest the Andreev reflection process with a finite barrier strength parameter  $Z$ . Thus the positions of the minima roughly reflect the SC gap value. This follows from the equations for the current-voltage characteristics

$$I(V) \sim \int_{-\infty}^{\infty} T(\epsilon) (f(\epsilon - eV) - f(\epsilon)) d\epsilon, \quad (1)$$

$$T(\epsilon) = \frac{2\Delta^2}{\epsilon^2 + (\Delta^2 - \epsilon^2)(2Z^2 + 1)^2}, \quad |\epsilon| < \Delta$$

$$T(\epsilon) = \frac{2|\epsilon|}{|\epsilon| + \sqrt{\epsilon^2 - \Delta^2}(2Z^2 + 1)}, \quad |\epsilon| > \Delta,$$

where  $f(\epsilon)$  is the Fermi distribution function. The broadening of the quasiparticle DOS in the superconductor can be taken into account if  $\epsilon$  will be replaced by  $\epsilon - i\Gamma$  in Eq. (1). We used Eq.(1) to fit the measured  $dV/dI$  curves of PCs and extract SC gap.

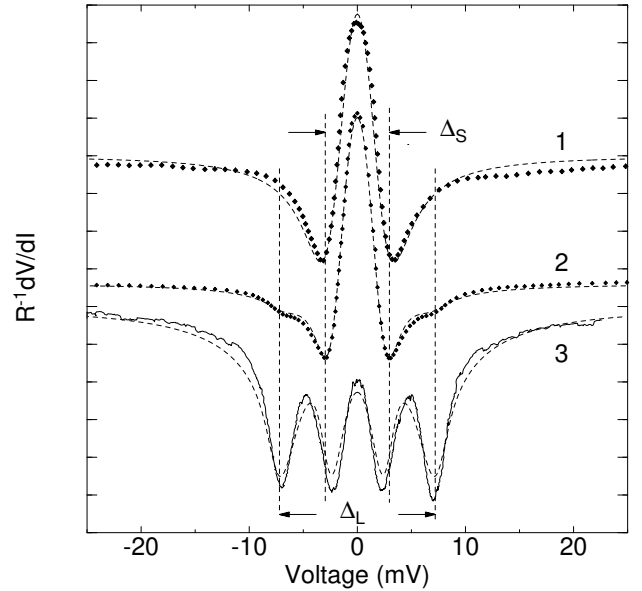


FIG. 1. Reduced differential resistance  $R_N^{-1}dV/dI$  vs.  $V$  measured for three MgB<sub>2</sub>-Ag contacts with one gap minima (curve 1,  $R_N=350 \Omega$ ) and two gaps (curve 2,3,  $R_N=20$  and  $\sim 25 \Omega$ ) structures. Symbol traces and bottom solid line are the experimental curves at  $T = 4.2$  K. Thin dashed lines are theoretical dependence calculated using Eq.(1) with one gap 2.7 meV (curve 1,  $Z=0.9$ ,  $\Gamma=1.2$  meV) and two gaps: 7.1 and 2.7 meV (curve 2,  $Z=0.9$ ,  $\Gamma=0.26$  meV), 7.4 and 2.6 meV (curve 3,  $Z=0.64$  and  $0.38$ ;  $\Gamma \simeq 0$ ). The gap weight factor ratio  $W_{Small}/W_{Large}$  is 10 and 1.5 for curves 2 and 3, respectively. The y-axis one division corresponds to 0.05 for curve 1 and 0.1 for curve 2.

<sup>1</sup>There is a scattering in  $\rho_0$  for the similar films between different publications [23,30,31].

The  $dV/dI$  curves taken at  $4.2\text{ K} \ll T_c$ , show usually minima around zero voltage at about  $\pm 2\text{--}3\text{ mV}$  with zero-bias maximum at  $V=0$  (see Fig. 1, curve 1), presumably related to the SC gap  $\Delta$ . Often the  $dV/dI$  vs.  $V$  curves show clear two gap structure with shallow features corresponding to a larger gap, as shown by curve 2 in Fig. 1. Among the many  $dV/dI$  curves (about 100), there was a curve 3 (Fig. 1) exhibiting almost equal features corresponding to the both gaps with minima at about  $\pm 7$  and  $\pm 2.3\text{ mV}$ . These values are close to the maxima at  $7$  and  $1.5\text{--}2\text{ mV}$  of gap distribution given in [20]. Fitting by Eq.(1) yields the correct gap value  $7.4$  and  $2.6\text{ meV}$ , which is consistent with  $7$  and  $2.8\text{ meV}$  from PC measurements in [19]. The larger gap to the lower one ratio  $2.85$  is close in our case to the theoretical value  $3:1$  [8].

### B. Phonons features

The voltage  $V$  applied to the ballistic contact defines the energy scale  $eV$  for scattering processes. EPI results in backflow scattering of energized electrons so that some of them are reflected by creating of phonons and do not contribute to the current. This leads to a nonlinear  $I - V$  characteristic and, as shown by the theory of Kulik, Omelyanchouk and Shekhter [32], second derivative  $d^2V/dI^2(V)$  of the  $I - V$  curve is proportional at low temperatures to  $\alpha_{PC}^2 F(\omega)$ :

$$\frac{d^2V}{dI^2} \propto R^{-1} \frac{dR}{dV} = \frac{8ed}{3\hbar v_F} \alpha_{PC}^2(\epsilon) F(\epsilon) \quad (2)$$

where  $\alpha_{PC}$ , roughly speaking, describes the strength of the electron interaction with one or another phonon branch and takes into account the kinematic restriction of electron scattering processes in the point contact by factor  $1/2(1 - \theta/\tan\theta)$  (for transport and Eliashberg EPI functions the corresponding factors are  $(1 - \cos\theta)$  and  $1$ , respectively), where  $\theta$  is the angle between initial and final momenta of scattered electrons. It should be mentioned that in PC the large angle  $\theta \rightarrow \pi$  scattering (back-scattering) processes of electrons are strongly underlined.

The PC resistance is determined by a sum of ballistic Sharvin and diffusive Maxwell term according to the simple formula derived by Wexler [34]:

$$R_{PC}(T) \simeq \frac{16\rho l}{3\pi d^2} + \frac{\rho(T)}{d}, \quad (3)$$

which is commonly used to estimate the PC diameter  $d$ . Here  $\rho l = p_F/ne^2$ , where  $p_F$  is the Fermi momentum,  $n$  is the density of charge carriers. The latter for

$\text{MgB}_2$  is estimated in  $n \simeq 6.7 \times 10^{22}$  [33], which results in  $\rho l \simeq 2 \times 10^{-12} \Omega \cdot \text{cm}^2$  using  $v_F \simeq 5 \times 10^7 \text{ cm/s}$  [4].

The measurements of  $d^2V/dI^2(V)$  dependencies to recover spectral EPI function reveal a wide variety of curves. Nevertheless, we were able to select similar  $d^2V/dI^2(V)$  characteristics for PC with different resistance (see Fig.2). The common features are the reproducibility of position of the main maxima placed at about  $40, 60$  and  $80\text{--}90\text{ meV}$  and lack of spectral features above  $100\text{ meV}$ . There is a correlation in the peak position in  $d^2V/dI^2(V)$  and calculated in [8] EPI function (Fig.2).

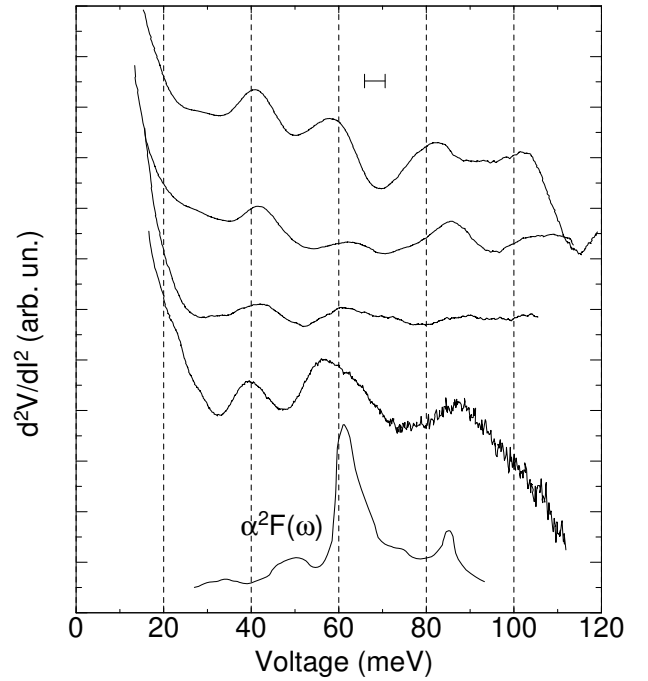


FIG. 2. Second derivative  $d^2V/dI^2(V)$  averaged for opposite polarities for 4  $\text{MgB}_2\text{-Ag}$  contacts with different resistance ( $R = 43, 36, 111$  and  $45\ \Omega$  from top curve to bottom one) at  $T=4.2\text{ K}$  with clear maxima in the range of phonons above  $30\text{ meV}$ . Bottom curve is calculated in [8] smoothed with experimental resolution (the segment above) EPI function. Signal increase in experimental curves below  $30\text{ meV}$  is due to the SC gap structure.

The mentioned features are seen also in the spectrum of another PC in Fig.3. Note, that this curve is measured in a magnetic field of  $4\text{ T}$ , which have to suppress additional features on  $d^2V/dI^2(V)$ , which could arise from SC weak links or degraded SC regions. It is also worth to be noted, that  $dV/dI(V)$  of this contact has an increase of resistance above  $30\text{ mV}$ , indicating a direct metallic contact. Absence of a non-superconducting layer at the interface <sup>2</sup> is confirmed by proximity induced supercon-

<sup>2</sup>Therefore, it is also reasonably to suggest for this con-

ductivity resulting in a sharp dip at  $V=0$  on  $dV/dI(V)$  (see Fig.3, inset).

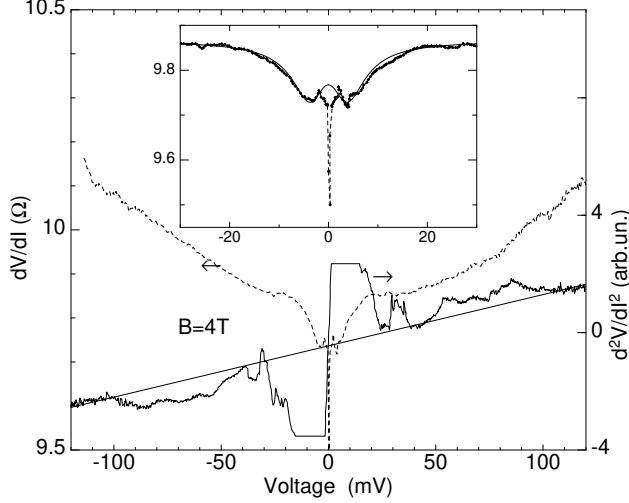


FIG. 3. First  $dV/dI(V)$  (dashed) and second  $d^2V/dI^2(V)$  (solid) derivative of  $I - V$  characteristics for  $\text{MgB}_2$ -Ag contact at 4.2 K and magnetic field 4 T. The  $d^2V/dI^2(V)$  curve is truncated near zero bias due to large signal caused by the SC gap. Straight line shows an approximate background corresponding to the parabolic shape of the first derivative. Inset demonstrates fitting of the  $dV/dI(V)$  (symbols connected by dashed line) by Eq.(1) (solid line). Parameters of the fit are:  $\Delta=3.8$  meV,  $Z=0.5$ ,  $\Gamma=3$  meV. Dip in  $dV/dI(V)$  at  $V=0$  is tentatively due to the proximity effect.

After subtracting a linear background, as shown in Fig.3, the presented in Fig.4 PC EPI spectrum (curves 1,2), has above 30 meV similarities with the phonon DOS measured by neutron scattering [9,10]. Below 30 meV all the spectra (see Fig.2,3) exhibit a steep increase connected with superconductivity (Andreev reflection). We have tentatively subtracted the nonlinear background in this region, as shown in inset of Fig.4, and found an intensive peak at 20 meV and around 30 meV (Fig.4). In principle, these peaks (as the other lower-frequency peaks not revealed yet) might not related directly to the EPI function, and could be due to, e.g., the suppression of the SC order parameter. This suppression can occur near the characteristic phonon energies with small group velocity, corresponding to peaks in phonon DOS, as observed for PC spectra of ordinary superconductor tanta-

lum [35]. Indeed, corresponding peaks may be found in the mentioned energy region at 16-17, 24, 31 meV [24,25] or hillock at 20 meV [9] in the phonon DOS determined by neutron scattering. Interesting, that PC EPI spectrum of pure Mg has also maxima at 17 and 28 meV (see Fig.4a)

As follows from the comparison of our data with the phonon DOS, all phonons above 30 meV contribute in average with approximately equal weight to the PC EPI function. We do not see the prevailing of one mode around 60-70 meV, as follows from calculated Eliashberg or transport EPI function in Ref. [5,6,8]. Probably, the reason is that our measurements are mainly along the c-axis.

Concerning the estimation of an absolute value of EPI function or EPI constant  $\lambda$  from PC data, it is still premature because the nonlinearity of PC  $I - V$  curves in the region of characteristic phonon frequencies is too low. As is seen from Fig.3,  $dV/dI$  increases above 30 meV only on a few percent contrary to 10-50% increase in the zero bias region due to the Andreev reflection at zero magnetic field. The short elastic electron mean free path in the constriction (diffusive regime) is likely the main reason of the small nonlinearity. Sure, to receive both quantitative results and final shape of EPI function the investigations of more perfect samples or even single crystals are very desirable.

tact that the barrier parameter,  $Z$ , obtained from the fit (see Fig.3, inset), is caused only by the mismatch of the Fermi velocities between the two electrodes. According to [29]  $Z = (1 - r)/2r^{1/2}$ , where  $r$  is the ratio of the Fermi velocities. Using the fitting parameter  $Z=0.5$  for this contact we find the Fermi velocity of  $\text{MgB}_2$  about  $5 \times 10^7$  cm/s taking  $1.4 \times 10^8$  cm/s as the Fermi velocity of Ag.

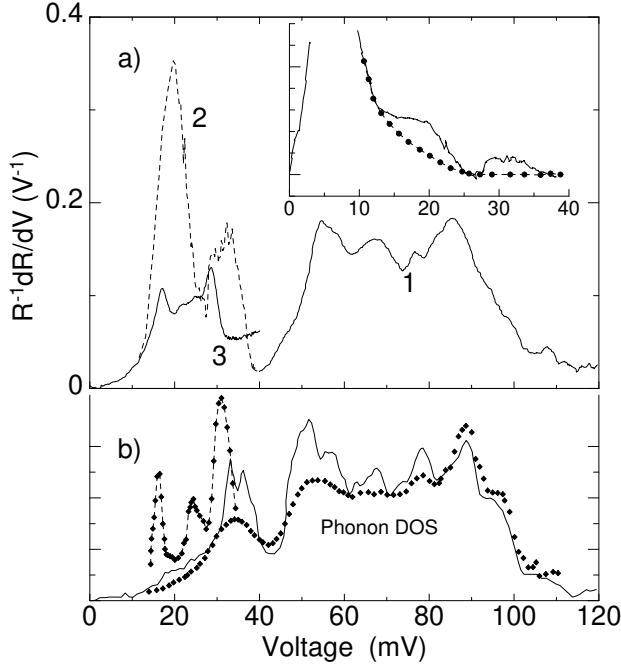


FIG. 4. a) PC EPI function (see Eq.(2)) of MgB<sub>2</sub> (curves 1 and 2) reconstructed from  $d^2V/dI^2(V)$  in Fig.3 averaging for plus and minus polarity after subtracting linear (as is shown in Fig.3) and hand-made (see inset) background. Solid curve (3) shows PC spectrum of pure Mg. Inset: proposed nonlinear background (symbols) below 30 meV for the same contact recorded with enlarged scale. b) Phonon DOS according neutron measurements [9](solid line), [10] (symbols) and [24] (symbols connected by dashed line). In the latter case only low energy (<40meV) part of phonon DOS is shown.

## II. CONCLUSION

Our results of investigation by point contacts the MgB<sub>2</sub> c-axis oriented thin film unequivocally indicate the presence of two SC gap with the theoretically predicted ratio 1:3 [8]. Above SC gap the EPI features dominate in the PC spectra. Thus the electron-phonon coupling in MgB<sub>2</sub> must therefore be included in any microscopic theory of superconductivity. The PC EPI function has similarities above 30 meV with the phonon DOS, while maxima at 20 and 30 meV are also resolved pointing that these low frequency phonon modes should be considered by describing of SC state of MgB<sub>2</sub>. Using the barrierless junction, the Fermi velocity  $5 \times 10^7$  cm/s in MgB<sub>2</sub> have been estimated.

## ACKNOWLEDGEMENTS

The work in Ukraine was supported by the State Foundation of Fundamental Research under Grant N02.07/00367. The work at Postech was supported by the Ministry of Science and Technology of Korea through the Creative Research Initiative Program.

- [1] J. Nagamatsu, N. Nakagawa, T. Muranaka, Y. Zenitani, J. Akimitsu, *Nature* **410**, 63 (2001).
- [2] S. L. Budko, G. Lapershot, C. Petrovic, C. E. Cunningham, N. Anderson, P. C. Canfield, *Phys. Rev. Lett.* **86**, 1877 (2001).
- [3] D. G. Hinks, H. Claus, & J. D. Jorgensen, *Nature* **411**, 457(2001).
- [4] J. Kortus, I.I. Mazin, K.D. Belashchenko, V.P. Antropov, L.L. Boyer, *Phys. Rev. Lett.* **86**, 4656 (2001).
- [5] Y. Kong, O. V. Dolgov, O. Jepsen, and O. K. Andersen, *Phys. Rev. B* **64**, 020501(R) (2001).
- [6] K.-P. Bohnen, R. Heid, and B. Renker, *Phys. Rev. Lett.* **86**, 5771 (2001).
- [7] J. M. An and W. E. Pickett, *Phys. Rev. Lett.* **86**, 4366 (2001).
- [8] A. Y. Liu, J. J. Mazin, and J. Kortus, *Phys. Rev. Lett.* **87**, 087005 (2001).
- [9] T. Yildirim, O. Gulseren, J. W. Lynn, C. M. Brown, T. J. Udovic, H. Z. Qing, N. Rogado, K.A. Regan, M.A. Hayward, J.S. Slusky, T. He, M.K. Haas, P. Khalifah, K. Inumaru, R.J. Cava, *Phys. Rev. Lett.* **87**, 037001 (2001).
- [10] R. Osborn, E. A. Goremychkin, A. I. Kolesnikov, and D. G. Hinks, *Phys. Rev. Lett.* **87**, 017005 (2001).
- [11] G. Karapetrov, M. Javarone, W. K. Kwok, G. W. Crabtree, D. G. Hinks, *Phys. Rev. Lett.* **86**, 4374 (2001).
- [12] G. Rubio-Bollinger, H. Suderow, S. Vieira, *Phys. Rev. Lett.* **86**, 5582 (2001).
- [13] A. Sharoni, I. Felner, D. Millo, *Phys. Rev. B* **63**, 220508R (2001).
- [14] C.-T. Chen, P. Seneov, N.-C. Yeh, R. P. Vasquez, C. U. Jung, M.-S. Park, H.-J. Kim, W.N. Kang, S.-I. Lee, *cond-mat/0104285*.
- [15] F. Giubileo, D. Roditchev, W. Sachs, R. Launy, J. Klein, *cond-mat/0105146*.
- [16] F. Giubileo, D. Roditchev, W. Sachs, R. Lamy, D.X. Thanh, J. Klein, S. Miraglia, D. Fruchart, J. Marcus and Ph. Monod, *cond-mat/0105592*.
- [17] H. Schmidt, J. F. Zasadzinski, K. E. Gray, D. G. Hinks, *Phys. Rev. B* **63**, 220504(R) (2001).
- [18] A. Plecenik, Š. Beňačka, P. Kúš, *cond-mat/0104038v2*.
- [19] P. Szabó, P. Samuely, J. Kacmarčík, Th. Klein, J. Marcus, D. Fruchart, S. Miragila, C. Marcenat, A. G. M. Jansen, *Phys. Rev. Lett.* **87**, 137005 (2001).
- [20] F. Laube, G. Goll, J. Hagel, H. v. Löhneysen, D. Ernst, T. Wolf, *cond-mat/0106407*.
- [21] A. Kohen and G. Deutscher, *Phys. Rev. B* **64**, 060506(R) (2001).
- [22] E. S. Clementyev, K. Conder, A. Furrer, and I. L. Sashin, *Eur. Phys. J. B* **21**, 465 (2001).
- [23] J. J. Tu, G. L. Carr, V. Perebeinos, C. C. Homes, M. Strongin, P. B. Allen, W. N. Kang, E.-M. Choi, H.-J. Kim, and S.-I. Lee, *cond-mat/0107349*.
- [24] T. Muranaka, S. Margadonna, I. Maurin, K. Brigatti, D. Colognesi, K. Prassides, Y. Iwasa, M. Arai, M. Takata

- and J. Akimitsu, J. of the Phys. Soc. of Japan **70**, 1480 (2001).
- [25] T.J. Sato, K. Shibata, and Y. Takano, cond-mat/0102468.
  - [26] D. Manske, C. Joas, I. Eremin, and K.H. Bennemann, cond-mat/0105507v2.
  - [27] S. V. Shulga, S.-L. Drechsler, H. Eschrig, H. Rosner, W. Pickett, cond-mat/0103154.
  - [28] I. K. Yanson, Sov. J. Low Temp. Phys. **9**, 343 (1983).
  - [29] G.E. Blonder, M. Tinkham, T. M. Klapwijk, Phys. Rev. B **25**, 4515 (1982).
  - [30] W.N.Kang, Hyeong-Jin Kim, Eun-Mi Choi, C.U.Jung, Sung-Ik Lee, Science **292**, 1521 (2001).
  - [31] H. H. Wen, S. L. Li, Z. W. Zhao, H. Jin, Y. M. Ni, W. N. Kang, Hyeong-Jin Kim, Eun-Mi Choi, and Sung-Ik Lee, Phys. Rev. B **64**, 134505 (2001).
  - [32] Kulik I. O., Omelyanchouk A. N. and Shekhter R. I. Sov. J. Low Temp. Phys. **3** 840 (1977).
  - [33] P.C. Canfield, D.K. Finnemore, S.L. Bud'ko, J.E. Ostenson, G. Lapertot, C.E. Cunningham, and C. Petrovic, Phys. Rev. Lett. **86**, 2423 (2001).
  - [34] A. Wexler, Proc. Phys. Soc. **89**, 927 (1966).
  - [35] I. K. Yanson, V. V. Fisun, N. L. Bobrov and L. F. Rybaltchenko, JETP Lett. **45**, 543 (1987).